frontiers | Frontiers in Earth Science

TYPE Original Research
PUBLISHED 27 December 2023
DOI 10.3389/feart.2023.1296459

OPEN ACCESS

EDITED BY
Hu Li,
Southwest Petroleum University, China

REVIEWED BY
Cunhui Fan,
Southwest Petroleum University, China
Cheng Zhong,
Nanjing Normal University, China

*CORRESPONDENCE
Yuanyu Yang,
yangyuanyu@petrochina.com.cn

RECEIVED 18 September 2023
ACCEPTED 27 October 2023
PUBLISHED 27 December 2023

CITATION
Yang Y, Li X, Wang Z and Yang W (2023), Tectonic movements of the Yanshan-Himalayan period in the northern Longmenshan and their impact on tight gas accumulation of the Shaximiao formation in the Qiulin structure, China. *Front. Earth Sci.* 11:1296459. doi: 10.3389/feart.2023.1296459

Tectonic movements of the Yanshan-Himalayan period in the northern Longmenshan and their impact on tight gas accumulation of the Shaximiao formation in the Qiulin structure, China

Yuanyu Yang[1,2]*, Xucheng Li[2], Zeqing Wang[1] and Wenbo Yang[1]

[1]College of Earth Sciences, Chengdu University of Technology, Chengdu, China, [2]PetroChina Southwest Oil & Gasfield Company, Chengdu, China

The Jurassic strata constitute a focal area for recent exploration and development of tight gas reservoirs in the western Sichuan Basin. This study investigates the Jurassic Shaximiao Formation in the northern Longmenshan in the Western Sichuan basin, focusing on tight gas reservoirs. The research integrates core and outcrop observations, seismic interpretations, and burial history analyses to understand hydrocarbon source rocks, sedimentation, reservoir characteristics, and structural characteristics. The impact of Yanshan-Himalayan tectonic movements on tight gas reservoir accumulation in the Shaximiao Formation is dissected, primarily around the Qiulin structure. The Western Sichuan Depression basin's formation is influenced by gravitational gliding tectonics, which can be classified into the 'Three Zones and One Belt,' with Longmenshan in the frontal belt. Burial history analysis reveals distinct processes in the foreland belt and the depression basin. In the Qiulin area, gas reservoirs in the Shaximiao Formation are mainly charged by source rocks from the Xujiahe Formation. Tectonic movements play a significant role in creating favorable reservoirs and conditions for hydrocarbon migration and preservation. Natural gas accumulation is primarily controlled by fault connectivity to hydrocarbon sources and effective reservoir thickness. Gravitational sliding tectonics have shaped a fluvial-lacustrine environment for the Shaximiao Formation, with fluvial sand bodies acting as favorable reservoir zones. Small-scale normal faults formed by tectonic movements serve as conduits for natural gas migration. The research findings are of significant guidance for the exploration and development of tight oil and gas resources in western Sichuan basin.

KEYWORDS

Longmenshan, tectonic movements, structural characteristics, tight gas, Shaximiao formation, gas accumulation, Qiulin structure

1 Introduction

The Longmenshan thrust belt is a vital transpressive zone in China, situated at the junction between the Pacific and Tethys-Himalayan tectonic domains. It forms part of the complex intracontinental foreland thrust system in central and western China, drawing significant attention from researchers worldwide due to its prominence in the study of thrust

belt tectonic deformation (He et al., 2022a; He et al., 2022b; Li et al., 2023). Geological research on Longmenshan began in the early 20th century and has yielded significant insights into its tectonic evolution, genetic models, uplift history, crustal structure, and deformation patterns. These accomplishments have advanced the understanding of thrust belt tectonic deformation theories and guided exploring and developing numerous large and medium-sized gas fields in western Sichuan (Yang et al., 2018; Xie et al., 2022; Yang et al., 2023a; Yang et al., 2023b; Xie et al., 2023). In recent years, significant oil and gas discoveries have been made in the northern Longmenshan foreland belt, particularly in the Shuangyushi structure. High-yield gas flows have been achieved from the Permian Qixia, Maokou Formations, and the Devonian Guanwushan Formation. The testing production capacity has reached as high as 126.77 × 10^4 m^3/d, showcasing the promising prospects for tight gas exploration in the northern Longmenshan (Deng et al., 2021; Ding et al., 2022). The primary exploration zones are situated within the northern and depression basin of the Longmenshan foreland belt, encompassing structures such as the Zitong, Bajiaochang, and Qiulin. The tectonic movements significantly influence aspects such as sedimentation, reservoir formation, migration, and accumulation (Yang et al., 2022).

The Sichuan Basin evolved from a paleo-uplift, and following the Jinning and Chengjiang movements in its early period, the basement folding in the basin area underwent reversion and cooled, leading to consolidation (Li et al., 2019; Gao et al., 2020; Liu et al., 2021). Consequently, the formation of a paleo-uplift began. The development of the Sichuan Basin can be divided into three periods. From the Cambrian to the Middle Triassic in the early period, a rift-related sedimentary basin with a cratonic marine environment was formed, primarily under extensional tectonic conditions. Carbonate rocks dominated the sedimentary deposits in this period. During the middle period, the Indosinian tectonic movement primarily influenced the Sichuan Basin. The basin was subjected to extensional tectonics, developing a series of large-scale normal faults. It resulted in the formation of a rifted basin, and during this period, the basin exhibited a phase of alternating marine and terrestrial environments. From the Jurassic to the Early Cretaceous, it experienced the Yanshan tectonic movement, manifesting as a subsidence basin. Starting from the Cretaceous, the basin underwent compressional forces due to the collision between the Longmenshan thrust belt and the rigid basement of the Sichuan Basin (Jin et al., 2009; Jin et al., 2010; Deng et al., 2018; 2018). It led to the formation of a foreland basin. As a result, the Sichuan Basin is predominantly the amalgamation of three major periods of basin evolution, leading to the development of a series of intricate structural patterns within its interior.

In the earlier periods of research, geological and structural studies in the northern Longmenshan primarily focused on the Xujiahe Formation and older strata. There has been limited investigation into the tectonic movements occurring after the Indosinian period. It only suggests a history of Yanshan uplift and strong Himalayan compression during the Yanshan-Himalayan tectonic phase. However, a detailed exploration of the Yanshan-Himalayan tectonic movements and associated structural characteristics remains insufficient. To a certain extent, this limited understanding has contributed to the lack of breakthroughs in oil and gas exploration in the Jurassic and overlying strata of the northern Longmenshan. The Shaximiao Formation exhibits extensive vertical development of fluvial sand bodies and a wide distribution in planar extent. It possesses favorable reservoir properties and significant exploration potential. Based on this, this study focuses on the Qiulin structure. An analysis of the Yanshan-Himalayan tectonic characteristics in northern Longmenshan aims to establish a definitive link between these movements and the tight gas accumulation of the Shaximiao Formation. The research offers guidance for developing tight gas reservoirs in the Sichuan Basin and oil and gas exploration in foreland basins.

2 Geological background

2.1 Tectonic setting

The Longmenshan thrust belt is a northeast-trending orogenic belt on the eastern Songpan-Ganzi highland. Regarding tectonic positioning, it lies along the western margin of the Sichuan Craton of the Yangtze Block. It is a convergence zone between the Yangtze Block, the North China Block, and the Indian Plate, presenting a predominant northeast to east-northeast orientation. In planar view, Longmenshan can be divided into the northern (from the north of Anxian to Guangyuan), the middle (from Huaiyuan to Anxian), and the southern (from Huaiyuan to the south of Ya'an) parts (Jin et al., 2009; Jin et al., 2010). It is primarily characterized by three regional and deep-seated faults: the Maoxian-Wenchuan Fault, the Yingxiu-Beichuan Fault, and the Pengguan Fault. These faults exhibit orientations consistent with the overall trend of the Longmenshan thrust belt (Figure 1A). Among them, the northern part is situated in the northeastern of the western Sichuan Depression. Influenced by the Tongwan Movement and the Late Caledonian Ancient Uplift, the northern thrust belt of the Longmenshan features a nearly complete sequence of Mesozoic, Paleozoic, and Ordovician strata (Deng et al., 2021). The area exhibits intricate structural complexity, marked by pronounced folding, with some local strata being nearly upright or even overturned. Simultaneously, a well-developed fault system is concentrated within the Devonian, Carboniferous, Permian, and Triassic formations above the Silurian strata. They often extend over considerable distances and are commonly associated with fractured zones. The Qiulin structure in the northern Longmenshan thrust belt has emerged as a focal area for oil and gas exploration in the western Sichuan region in recent years (Figure 1A). Significant discoveries have been made, particularly in formations such as the Shaximiao Formation, which represents tight gas reservoirs.

2.2 Stratigraphy

In the northern Longmenshan, the exposed surface strata predominantly include Jurassic, Permian, Triassic, Carboniferous, Devonian, Silurian, and Cambrian formations. The Middle and Late Cambrian, Ordovician, and Late Carboniferous strata are absent (Lei et al., 2012; Wu et al., 2012). The Permian formations are primarily situated near the core of the Tianjingshan anticline, with a thickness of approximately 460–600 m. The lithology predominantly

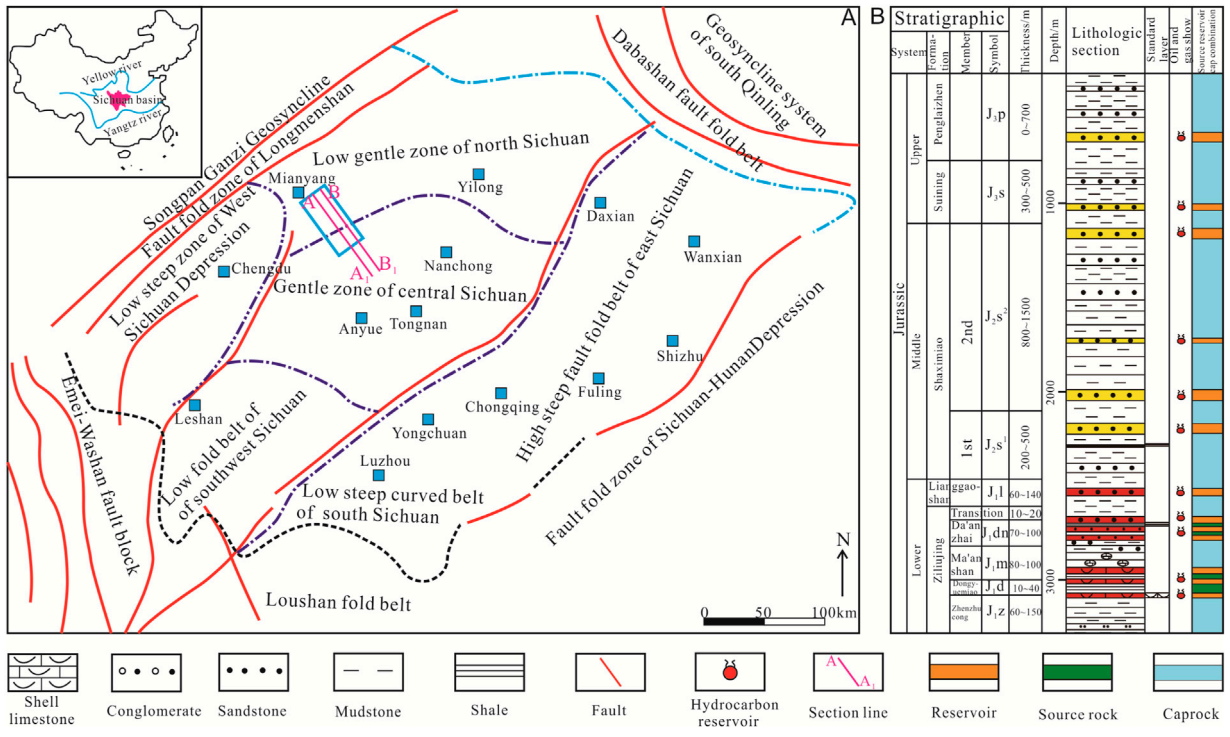

FIGURE 1
Geological setting of the study area. **(A)** The structural position of the study area; **(B)** Stratigraphic and lithological characteristics of the Shaximiao Formation (modified from Li et al., 2019a; Li et al., 2019b; Wei et al., 2021).

comprises carbonate rocks, with only the base of the Liangshan and Wujiaoping formations containing coal-bearing sand and mudstones. The Triassic formations are found on the western and northern Tianjingshan anticline, with an exposed thickness of approximately 1,000–2,500 m. The lithology is predominantly characterized by carbonate rocks, with the Feixianguan and Xujiahe formations containing predominantly terrestrial clastic rocks. The Carboniferous and Devonian formations are only exposed in the higher parts of the anticline's core and the northwest flank. The Carboniferous formation consists of approximately 70 m of carbonate rocks. The Devonian formation can be divided into upper, middle, and lower members. The lower member comprises sandstone with a thickness of around 150 m, while the middle to upper members primarily consist of marine carbonate sedimentation. The Cambrian strata are sparsely exposed in the core of the anticline, predominantly characterized by clastic rocks. The primary target reservoir of the Qiulin structure is the Jurassic Shaximiao Formation. It consists of a thick sequence of fluvial-dominated sand-mudstone sedimentation, with a thickness ranging from 800 to 2,200 m (Wei et al., 2021; Lu et al., 2022). The deposition pattern is characterized by thinning towards the southwest and thickening towards the northeast. The Shaximiao Formation is divided into two members (1st and second) based on the "Estheria shale" (Figure 1B). The 1st Member has a thickness of approximately 900–1,000 m. The Estheria shale marks its base, and the bottom of the brick-red feldspathic sandstone of the Suining Formation defines its top. This member consists of a purple-red to dark purple-red mudstone interbedded with thick layers of blocky sandstone, with sandstone thickness ranging from 10 to 20 m. It is the primary focus for exploration and development within the Qiulin structure.

3 Data and methods

3.1 Samples and data

This study focuses on the Qiulin structure as the primary analysis area, employing detailed structural interpretation and analysis of reservoir-forming processes. It aims to analyze the impacts of multiple tectonic movements during the Yanshan-Himalayan period on sedimentation, reservoir formation, oil and gas migration, and preservation of the Jurassic Shaximiao Formation in the northern of the Longmenshan and ascertain its controlling role in the accumulation of natural gas. This study's main samples and data include field investigations of 20 outcrop profiles, core observations and drilling data from 5 wells, 3D seismic data covering an area of 100 km^2, conventional and imaging logging data from 5 wells. Core observations and logging data are primarily employed to study sedimentary and reservoir characteristics. Drilling and seismic data are primarily utilized for constructing subsidence history curves. When combined with outcrop features, these data aid in analyzing periods of tectonic movement, providing a basis for structural evolution analysis. The 3D seismic data is employed for detailed structural interpretation, analyzing the tectonic movements and structural characteristics, and establishing the relationship

between structures and gas accumulation. Additionally, data on the main source rocks, sedimentation, stratigraphy, and lithological characteristics of the study area have been collected.

3.2 Methods

3.2.1 Sedimentation history analysis

The sedimentary basin experiences different tectonic movements, resulting in distinct subsidence mechanisms. As a result, the subsidence magnitude and characteristics of subsidence curves also exhibit significant variations. Subsidence can typically be categorized into structural and total subsidence, with this study primarily focusing on the former.

3.2.1.1 Normal compaction model (Overburden deformation calculation)

Previous research findings have revealed that under normal pressure conditions, there exists an exponential relationship between sediment porosity and depth (Xia et al., 2018).

$$\phi(z) = \phi_0 e^{-c^* z} \tag{1}$$

Where: z represents the burial depth of sediment, $\phi(z)$ stands for the porosity of the sediment at depth z, ϕ_0 is the initial porosity of the sediment deposit, and c denotes the sediment compaction constant, reflecting the gradient of porosity change with depth.

Since a geological profile can be divided into several units, a unit could represent a geological interval characterized by sediment types such as sandstone, mudstone, limestone, dolomite, chalk, gypsum, and other lithologies. Hence, calculations based on formula (1) are performed for different lithologies separately while considering the proportions of various lithologies present within each unit.

The terrestrial strata in the study area are primarily composed of sandstone and mudstone. The calculation method for these is as follows:

$$\phi(z) = r_{sh}\phi_{osh} e^{-Csh^* z} + (1 - r_{sh})\phi_{os} e^{-Cs^* z} \tag{2}$$

Where: r_{sh} is the content of mudstone, ϕ_{osh} and ϕ_{os} are the initial porosities of mudstone and sandstone, respectively, C_{sh} and C_s are the compaction coefficients for mudstone and sandstone, respectively.

3.2.1.2 Paleothickness restoration model (backstripping calculation)

Once the porosity-depth relationship is established, the stratigraphic thickness data for different periods on current strata can be used to restore the burial paths of each layer since deposition.

3.2.1.3 Backstripping Model for continuous sedimentary profiles

For continuous sedimentary geological profiles, according to the principle of "tectonic skeleton invariance," the burial depths of various sedimentary layers during different geological epochs can be restored using present-day stratigraphic data (Martins et al., 2023).

$$\int_{Z_1}^{Z_2} 1 - \phi(z) dz = \int_{Z_{1a}}^{Z_{2b}} (1 - \phi(z)\backslash) dz \tag{3}$$

Where: z_1 and z_2 represent the present-day burial depths of the bottom and top boundaries of the current stratum. z_{1a} and z_{2b} represent the burial depths of the bottom and top boundaries of the current stratum during a certain geological epoch.

3.2.1.4 Backstripping model for profiles with erosional surfaces

When strata undergo erosion, the porosity-depth relationship changes, and its calculation formula is as follows:

$$\phi_B = e^{-c(h+s)} \tag{4}$$

The skeletal thickness of the eroded layer before restoration is:

$$H_B = \int_{Z_1}^{Z_2} [1 - \phi(z)] dz \tag{5}$$

After erosion restoration, the skeletal thickness of the eroded layer becomes:

$$H_B = \int_{Z_1}^{Z_2} [1 - \phi_B(z)] dz \tag{6}$$

The restoration of paleo thickness for each geological period still follows the principle of tectonic skeleton invariance, thus determining the burial history of the geological stratum.

$$\int_{Z_1}^{Z_2} [1 - \phi_B(z)] dz = \int_{Z_{1a}}^{Z_2{}^b} [1 - \phi_B(z)] dz \tag{7}$$

For the strata below the erosional layer, the process involves calculating the skeletal thickness based on current burial depths. Then, paleo thickness during various geological periods is computed using the porosity-depth relationship restored after erosion. As for the strata above the erosional layer, the procedure is the same as that for continuous sedimentary profiles.

3.2.1.5 Basin subsidence history model

For the sake of simplicity, this study's subsidence history model disregards the inherent strength of the lithosphere and employs a straightforward subsidence history model under the assumption of local Airy isostasy (equilibrium equation) (Zhang et al., 2009). The calculation formula is as follows:

$$Y = \frac{S^* (p_m - p_s)}{(p_m - p_w)} - \frac{\Delta SL^* p_w}{(p_m - p_w) - (W_d - \Delta SL)} \tag{8}$$

Where S is the sediment thickness adjusted for compaction, P_m, P_w, and P_s represent the mantle, water, and sediment densities, respectively, ΔSL is the amplitude of sea level change, and W_d is the paleowater depth.

3.2.2 3D seismic data processing

To thoroughly investigate the structural characteristics of the Qiulin area, delineate its structural morphology, and identify potential trap targets, a research approach was employed that transitioned from analyzing individual points to studying linear features and then further to examining broader geological patterns. This approach involved utilizing well logging and 3D seismic data as a foundation, building upon regional comprehensive research findings, and employing methods such as well-seismic correlation, integration of various cross-sections and profiles, to conduct a detailed interpretation of structural characteristics (Figure 2).

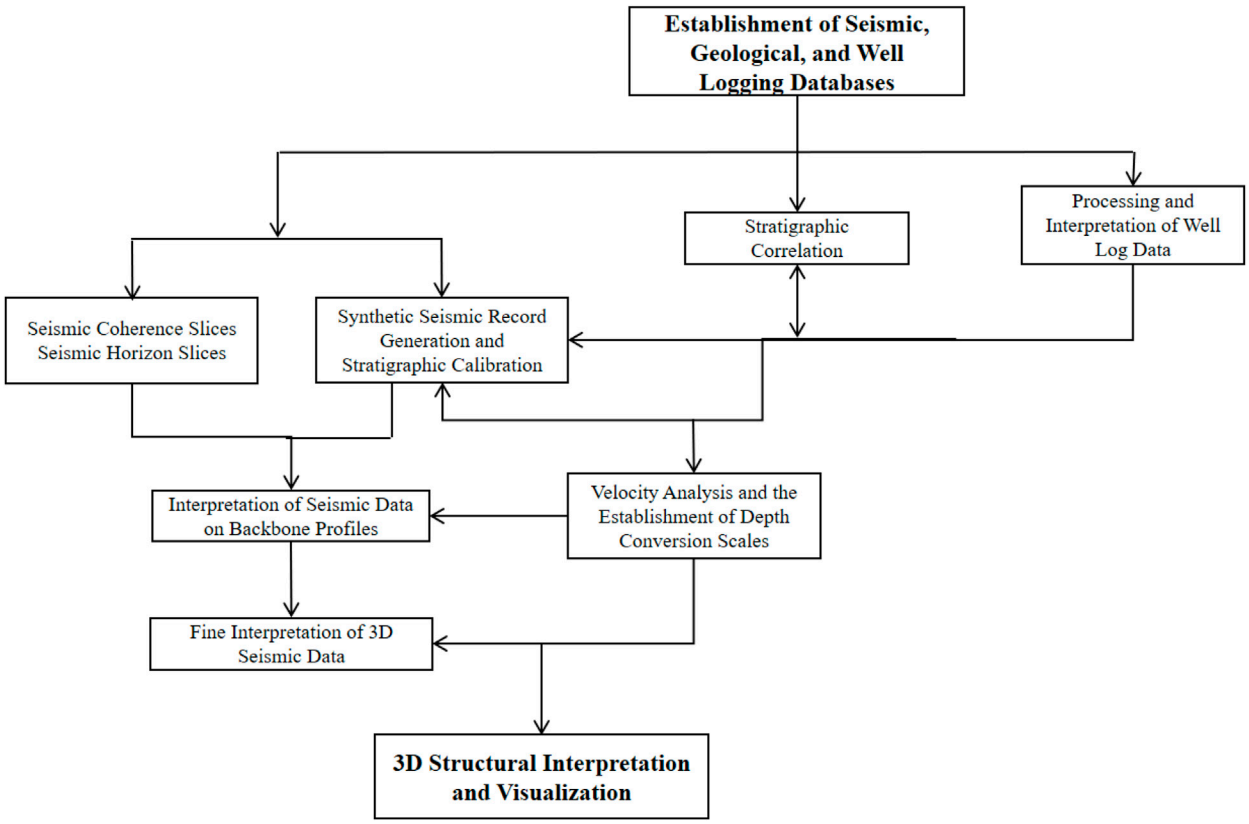

FIGURE 2
Schematic diagram of the 3D seismic structural interpretation process.

The process can be broken down into three steps: 1) Fine stratigraphic calibration and profile establishment: This involves establishing main cross-sections and analyzing seismic waveform characteristics through detailed stratigraphic calibration. 2) Interpretation of faults using coherent bodies, bed dip, and time slices combined with seismic profiles. This ensures spatial closure of faults in the study area, enabling a detailed understanding of fault profile and planar characteristics. 3) Progressive interpretation based on actual needs: Interpretation is intensified to accurately depict local structural styles and features, leading to a precise characterization. These steps culminate in a comprehensive analysis of structural characteristics, utilizing techniques such as well-seismic correlation, cross-section integration, and seismic data to create a thorough understanding of the geological formations in the Qiulin area.

4 Results

4.1 Characteristics of source rocks

The Middle to Upper Jurassic of the Sichuan Basin is primarily characterized by secondary hydrocarbon reservoirs, with the main source rocks originating from the Triassic Xujiahe Formation and Early Jurassic strata (Dai et al., 2009; Mu et al., 2019; Wu et al., 2023). Through comparative analysis of the gas source from the 1st member of the Shaximiao Formation, it is evident that the predominant gas source is mature coal-derived gas, followed by mixed sources of mature oil and coal, primarily originating from the underlying Xujiahe Formation and Jurassic source rocks (Figure 3) (Dai et al., 2009). The source rocks of the Xujiahe Formation are generally characterized by moderate to high maturity, with vitrinite reflectance ranging from approximately 0.4%–0.6% and temperatures around 500 °C. The maturity decreases gradually from the western to the eastern Sichuan Basin. The Jurassic source rocks primarily consist of organic-rich lacustrine deep-gray and black mudstones. These source rocks exhibit greater thickness in the central, northern, and eastern Sichuan basins while gradually thinning towards the western and southern Sichuan basin (Freeman et al., 1990; Wang et al., 2023). Overall, the thickness of the source rocks is generally over 50 m, with the maximum thickness reaching up to 380 m. The organic carbon content ranges from 0.03% to 32%, with an average of 0.96%. The kerogen is classified as Type II_2. Controlled by two major hydrocarbon generation centers, the Jurassic Xujiahe Formation in central Sichuan exhibits strong hydrocarbon generation (Li et al., 2022; Ma et al., 2023). Through hydrocarbon-bearing faults, the underlying natural gas can effectively charge the tight gas reservoirs of the Shaximiao Formation.

4.2 Sedimentary characteristics

In the early Jurassic, as the tectonic activity of the Longmenshan in western Sichuan gradually weakened, the Micashan-Dabashan

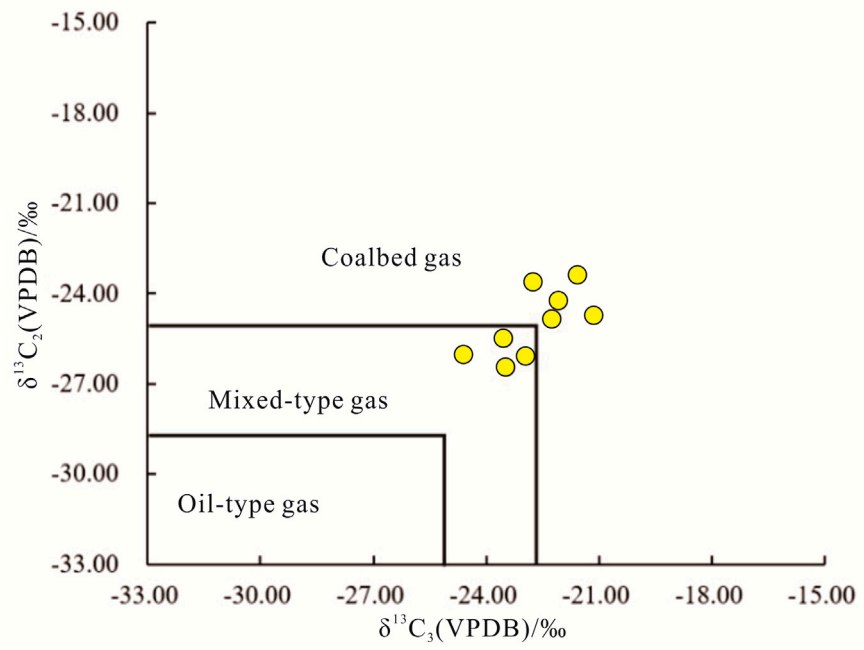

FIGURE 3
Carbon isotopes of the gas reservoir in the 1st Member of the Shaximiao Formation (see data in Dai et al., 2013; Dai et al., 2018).

tectonic zone in northern Sichuan responded to the subduction of the North China Plate and began to be active (Huang et al., 2022). As a result, the sedimentary center shifted from the western towards the northern and northeastern of the Sichuan Basin. During this period, there were two significant phases of basin expansion (Luo et al., 2013). The expansion of the basin was most extensive during the deposition of the Da'anzhai Formation, covering the areas of the eastern, northern, and central Sichuan Basin. This expansion exhibited a gradual transition from deep to shallow conditions. The deep-lake facies were present in the northeastern Sichuan Basin, particularly around the Dazhou-Wanzhou area. In contrast, in the basin regions closer to the mountain belt, sedimentation is primarily characterized by deltaic, fluvial, and alluvial fan deposits, representing a transition from the mountainous areas towards the basin.

During the Middle Jurassic Lianggaoshan Formation deposition period (referred to as the Xintiangou Formation in the Hechuan area and Qianfoya Formation in northern Sichuan basin), the sedimentary center was primarily situated in the Wangcang of the northern Sichuan to the Dazhou and Tongjiang of the northeastern Sichuan. A fan delta-lake sedimentary system existed in the northern part, while a fluvial-delta sedimentary system was prevalent in the southern and western parts (Wen et al., 2017). After the Upper Shaximiao Formation deposition, the Sichuan Basin evolved into a continental shallow-water basin. The water body was relatively shallow, and oxidation processes were prominent. The lithology consists of thick alternating layers of purplish-red and grayish-green sandstone and mudstone. During the late period of the Early Shaximiao Formation deposition, there was a significant and rapid rise in the lake level, leading to basin expansion. In the central to western Sichuan Basin, there is a widespread occurrence of black shale containing abundant leafy brachiopods at the top of the Lower Shaximiao Formation, commonly referred to as "Estheria shale." Simultaneously, during this period, the basin area gradually decreased once again. In the northwestern and northern parts of western Sichuan, the foreland areas exhibited fluvial sedimentation, while in the southern foreland of the mountain belt, there was mainly alluvial fan sedimentation transitioning to fluvial deposition (Figure 4).

Overall, during the sedimentation period of the Shaximiao Formation, tectonic activity was minimal, sedimentation was relatively gentle, and arid conditions characterized the environment. The Shaximiao Formation predominantly comprises a dark purple-red mudstone interbedded with gray-green and gray-white sandstone through the outcrop, core, logging, and seismic analysis. Based on the 'Estheria shale' as a boundary, it is divided into two members. The 1st Member has a thickness ranging from 200 to 300 m, and the second Member is 900–1,100 m. During the deposition of the 1st Member, the Qiulin structure developed a river-lake depositional system. Based on core observations from wells such as QL 16, QL 17, QL 202, and QL 205, a thick succession of blocky, extensive gray, medium-to fine-grained feldspathic sandstone beds representing channel sand bodies have been identified. These sand bodies exhibit a relatively pure sandy composition, with upward fining of grain size. The cores commonly display low-angle cross-stratification. Prominent scour surfaces are evident at the base of the sand layers, and the upper portions of these scour surfaces show sandstone beds containing mud and gravel, with gravel diameters reaching up to approximately 10 cm. This indicates deposition within a relatively high-energy fluvial channel environment. Therefore, the second Member in the study area represents meandering river deposition. The second Member can

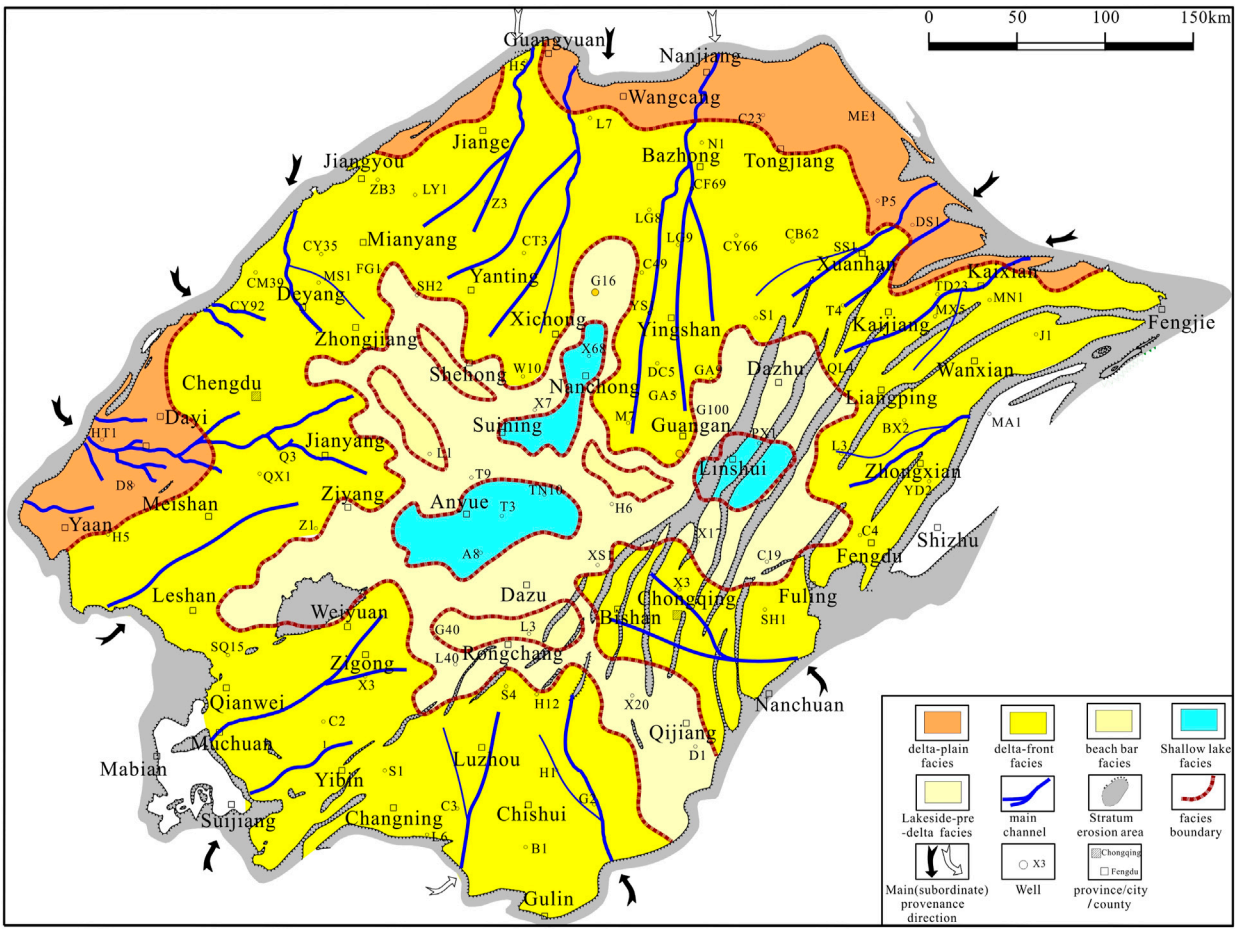

FIGURE 4
Sedimentary facies of the 1st Member of the Shaximiao Formation in the Sichuan basin.

be subdivided into four sub-members. Among these, one to three sub-members exhibit abundant sediment supply and the development of large-scale isolated sand bodies. 4 sub-member is characterized by alluvial plain sedimentary facies, which is not a favorable zone for reservoir development.

4.3 Reservoir characteristics

Tectonic movements primarily influence reservoir lithology and petrophysical properties through sediment supply. The sediment provenance in the study area is controlled by the tectonic movements of the northern Longmenshan and the Dabashan-Micangshan area, mainly originating from the northwest and northeast directions (Yu et al., 2021; Liu et al., 2023; Lyu et al., 2023). According to observations of detrital grains, cores, and thin sections, the reservoir of the second Member is predominantly composed of medium-grained lithic feldspathic sandstone (Figure 5A). The sorting is moderate to good, with subangular to subrounded grain shapes, and particle contacts are mainly point-to-line.

Based on core samples analysis from 5 wells, reservoir porosity ranges from 6% to 14%, with an average of 11.3%. Permeability is primarily distributed between 0.01 and 1 mD, with an average permeability of 0.43 mD. Sands developed during the same period exhibit similar reservoir petrophysical conditions, and porosity and permeability are positively correlated. This allows for qualitatively classifying the reservoir in this area as porous (Figure 5B). The T_2 relaxation spectrum of the second Member primarily exhibits a bimodal distribution, with an overall left-high and right-low pattern (78%) (Figure 5C), indicating a relatively higher content of small-sized pores (Gu et al., 2021; Xu et al., 2022; Yang et al., 2023c). Most samples exhibit a distinct left peak higher than the right peak, with an average T_2 cutoff value of 3.3 ms. This signifies that the reservoir samples in the study area possess small pore apertures and limited pore connectivity. Mobile fluids within the rock's pore-throat spaces are scarce, resulting in intricate pore structures forming during subsequent diagenetic processes.

4.4 Characteristics of tectonic movement

4.4.1 Tectonic characteristics during the Yanshan-Himalayan period

4.4.1.1 Analysis of depositional history

We conducted burial and subsidence history analysis on 9 wells in the study area using mud logging, logging data, and sedimentary

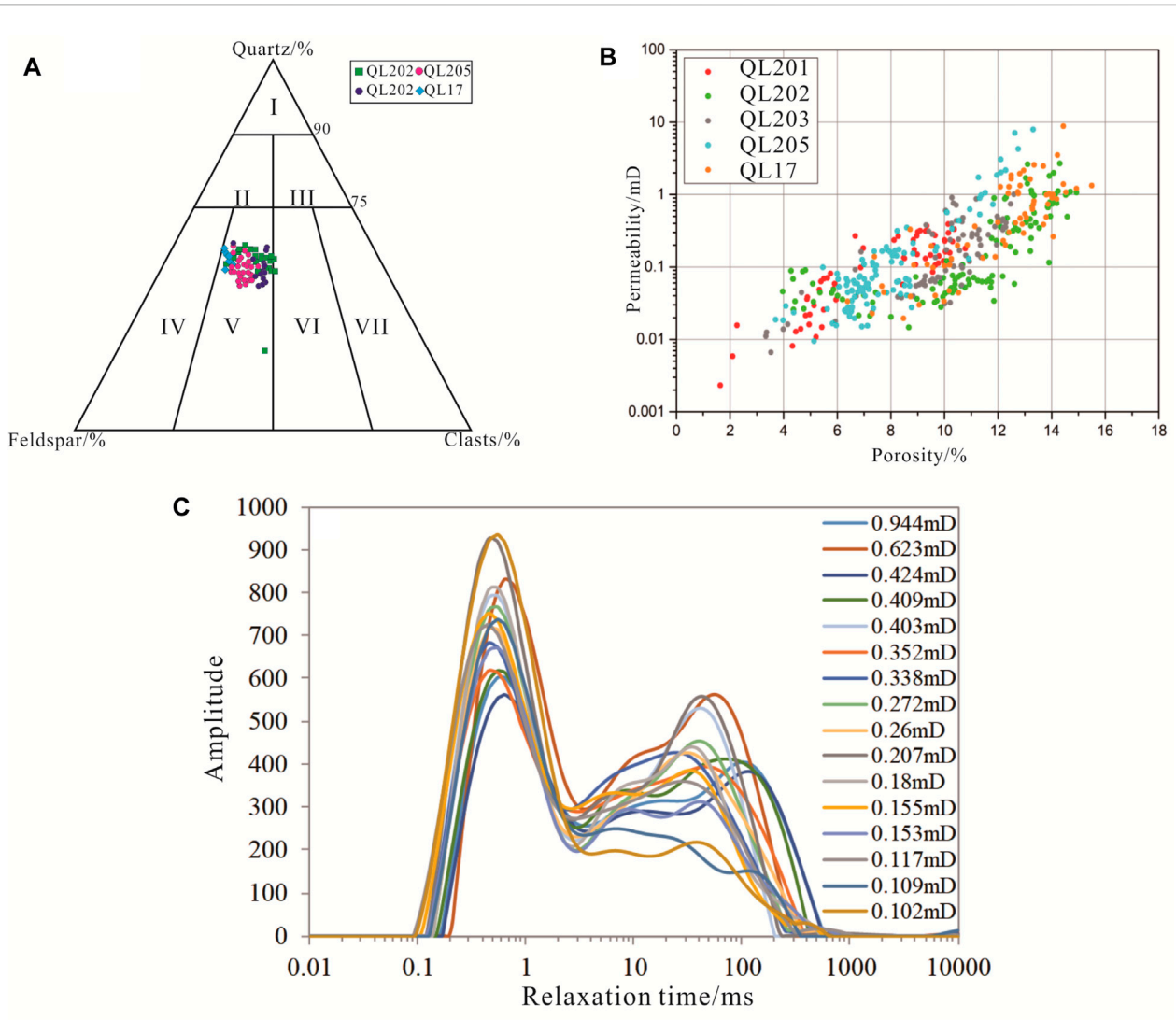

FIGURE 5
Basic reservoir characteristics of the second Member of the Shaximiao Formation. **(A)** Petrographic characteristics; **(B)** Reservoir petrophysical properties; **(C)** T_2 spectrum distribution of the core samples.

history calculation methods. Among them, 1 well (HX 1) is located in the frontal zone of the northern Longmenshan, 3 wells (Z18, Y1, and H2) are located in the frontal area, and 3 wells (W1, GJ1, SY1, and L1) are located within the basin (Figure 6A). Based on the subsidence curve analysis, it is believed that the frontal zone of the northern Longmenshan experienced a sequence of subsidence phases during the Jurassic period, which can be divided into "rapid subsidence - slow subsidence - rapid subsidence - intense uplift" phases. The sedimentary evolution of the northern frontal zone of Longmenshan and the intrabasinal area during the Jurassic is characterized by a sequence of subsidence phases: "rapid subsidence - slow subsidence - rapid subsidence - slow subsidence - rapid uplift." Compared to the frontal zone, the sedimentary history of the frontal and intrabasinal areas includes an additional Cretaceous sedimentation phase, and the influence of the Himalayan uplift during that period is relatively minor (Figure 6). The varying sedimentary history curves in different areas indicate that they were subjected to distinct tectonic settings during the same period, leading to differential subsidence and accommodating varying degrees of sedimentation (Alsalem et al., 2017; Zhu and Li, 2019; Petermann et al., 2022). The study area can be primarily categorized into frontal belt and foreland-basin sedimentary types. Despite sharing the same tectonic background, the different forms of tectonic activity have led to distinct subsidence history curves.

The subsidence history curve of the frontal belt exhibits a pattern of "rapid subsidence-slow subsidence-rapid subsidence-intense uplift," indicating that this area experienced rapid subsidence during the Early Jurassic, followed by a sustained period of slow subsidence during the Early to Middle Jurassic (Figure 6B). During the Late Jurassic to Early Cretaceous, the backside of Longmenshan experienced another rapid uplift, leading to intense subsidence in the frontal belt. This subsidence resulted in the deposition of a thick layer of conglomerates belonging to the Lianhuakou Formation. During the Late Cretaceous of the Yanshan period, the intensified tectonic activity led to rapid uplift of the entire northern Longmenshan. The frontal belt of the mountain, where Jurassic

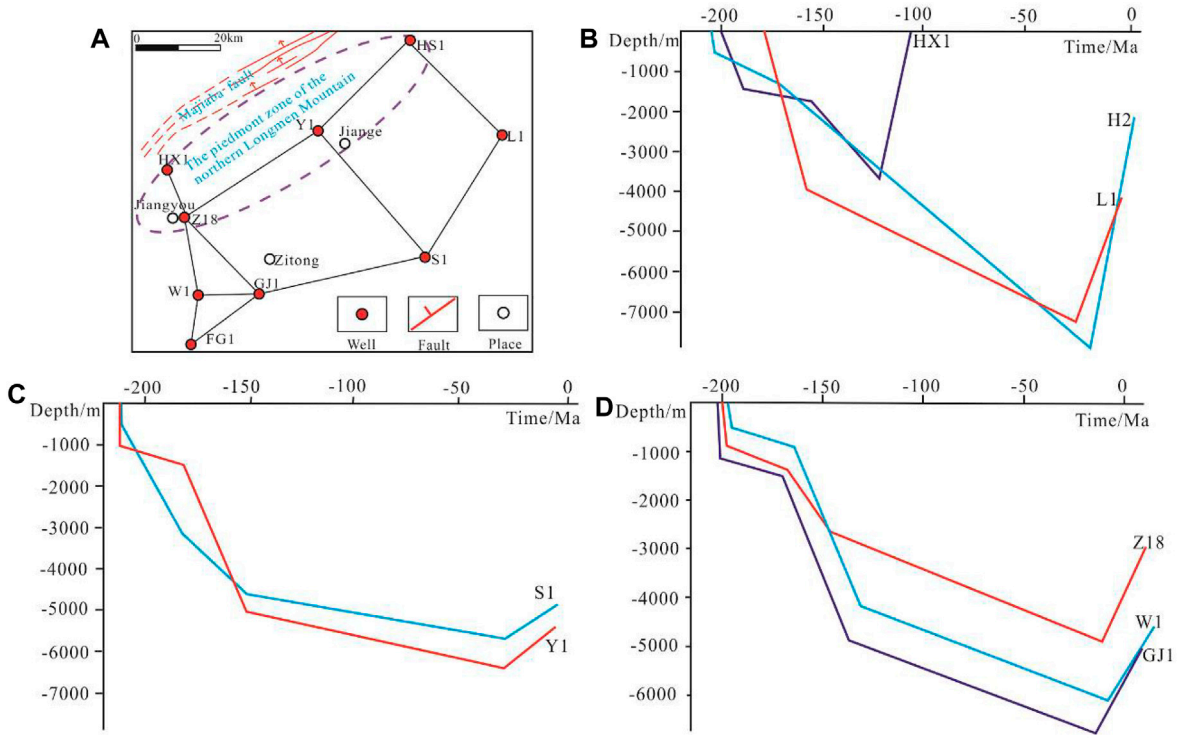

FIGURE 6
Depositional history curve of Jurassic in the foreland belt of the Longmenshan-Northwestern Sichuan Basin. **(A)** Relative position of the wells; **(B)** HX1, L1, and H2 wells; **(C)** S1 and Y1 wells; **(D)** Z18, W1, and GJ1 wells.

strata were previously exposed, was uplifted and exposed to the surface. Entering the Late Yanshan period, tectonic activity intensified, significantly uplifting the northern Longmenshan. The foreland belt of the mountain, where Jurassic strata were exposed, emerged above the water surface. The overlying Cretaceous Jianmenguan Formation was subsequently deposited atop the underlying Lianhuakou Formation. At the base of the Jianmenguan Formation, a sequence of conglomerates indicative of alluvial fan deposition was laid down. Following this phase, no new sedimentary strata were added to the foreland belt. As the Himalayan tectonic movement commenced, the foreland belt continued to experience uplift and underwent erosion.

The foreland-basin sedimentary history curve exhibits the characteristics of "rapid subsidence-slow subsidence-rapid subsidence-slow subsidence-violent uplift," indicating that the area experienced rapid subsidence during the Early Yanshan period (Figures 6B–D), followed by a sustained slow subsidence process from Early to Middle Yanshan. By the Middle-Late Yanshan period, the back ridge of Longmenshan experienced another rapid uplift, leading to intense subsidence in the foreland belt. This subsidence resulted in the deposition of a thick sequence of the conglomerates Jurassic Lianhuakou Formation and Cretaceous Jianmenguan Formation. Subsequently, the area underwent slow subsidence, leading to the deposition of the middle and upper parts of the Cretaceous strata. As the Himalayan began, the northern Longmenshan was rapidly folding and uplifting. In this area, there is an absence of Tertiary sedimentary strata. Sedimentary evidence is only present in the southern foreland basin, particularly in the Ya'an-Mingshan area.

The inflection points in the tectonic subsidence curve (indicating changes in subsidence rates) correspond closely to significant events in the geological evolution of the study area. The curve's starting point corresponds to the period of uplift of the hinterland of the northern Longmenshan and the thrust belt during the Yanshan orogeny (Figures 6B–D). The first inflection point marks the transition from intense activity to a relatively calm period. The second inflection point indicates that the curve steepens again, signifying the transition from a quiet period to intense tectonic activity during the Middle-Late Yanshan. The third inflection point shows a rapid increase, representing the intense tectonic activity and rapid uplift of the strata during the Late Yanshan in this area.

4.4.2 Structural characteristics of the foreland belt in the northern Longmenshan

4.4.2.1 Gravity sliding tectonic system

Gravity sliding deformation is typically considered a systemic structural deformation and displacement process, primarily driven by the uplift of the hinterland, causing the development of slopes (Bretas et al., 2012; Braunagel et al., 2023). Under gravity, rock layers slide downward to lower positions, forming a series of structural patterns. We divide it into four distinct zones: the uplifted zone, the slope zone, the frontal zone, and the depressed area. Gravity sliding systems exhibit mainly two thrust-style and wedge-style deformations. The most intense deformation occurs at the frontal portion of the thrust-style deformation (such as the Longmenshan thrust belt), where

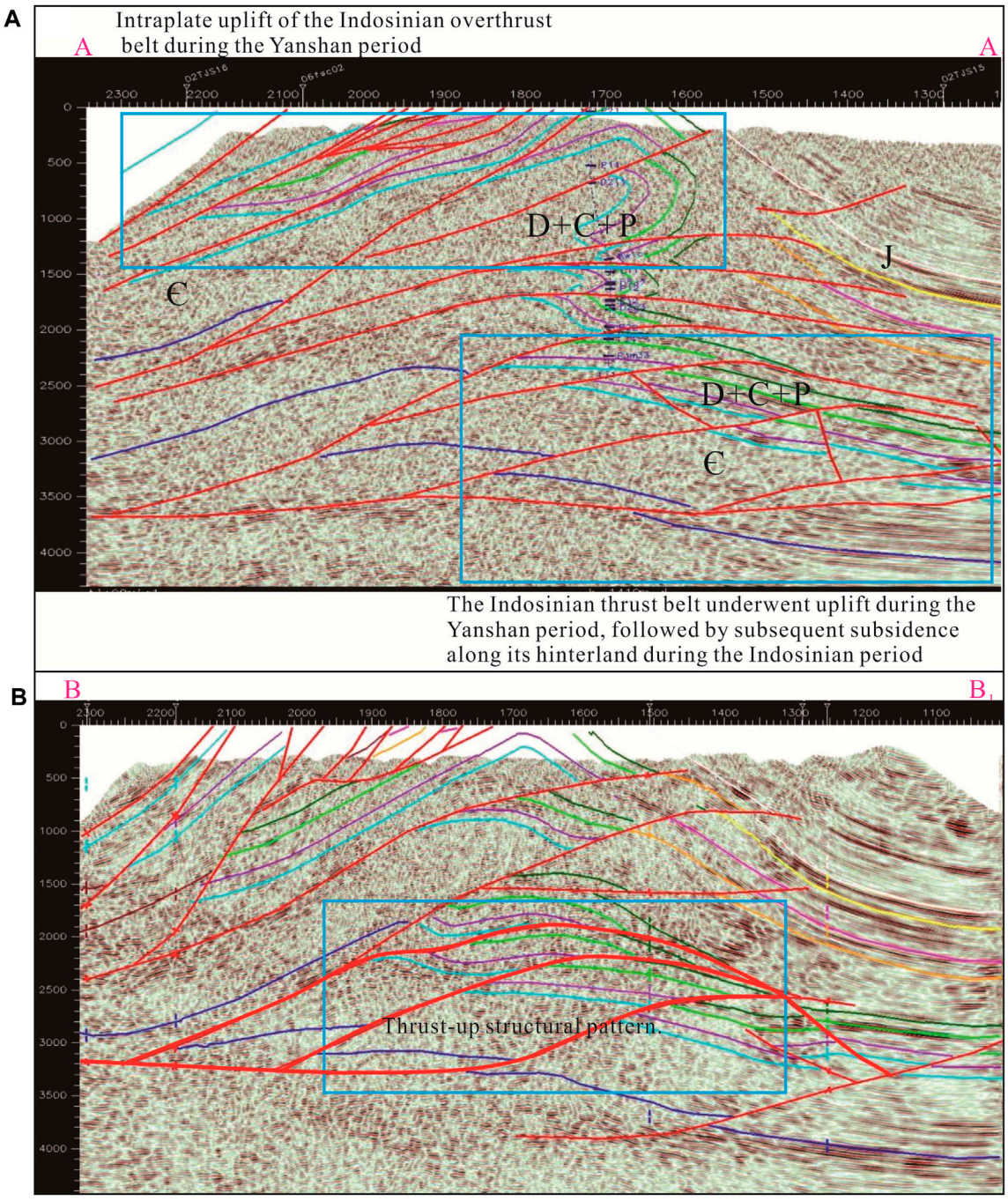

FIGURE 7
Seismic profile characteristics of gravity sliding structural system. **(A)** Structural pattern of gravity sliding foreland-style; **(B)** Thrust-up structural pattern.

deformation diminishes notably toward the rear, characterized by overall uplift (as seen in the Songpan-Ganzi highland). The central area demonstrates a large transitional slope zone (along the rear of the Longmenshan thrust belt).

In the western and central parts of the study area, the structural characteristics exhibit a typical gravity sliding foreland-style pattern. During the Indosinian-Yanshan period, these structures were influenced by gravity sliding within a compressional tectonic dynamic environment. They interacted with the rigid basement of the Sichuan Basin, resulting in intense rock deformation and the development of a series of thrust faults (Figure 7A) (Gunderson et al., 2018). In contrast, the shallow-level structures display a relatively gentle configuration, predominantly influenced by sedimentation. The intensity of tectonic deformation and displacement gradually diminishes towards the depocenter area. Due to the significant influence of the main fault on the deformation of the strata, exceeding their capacity to withstand, results in the development of disruptive faults in the rock layers, which release stress.

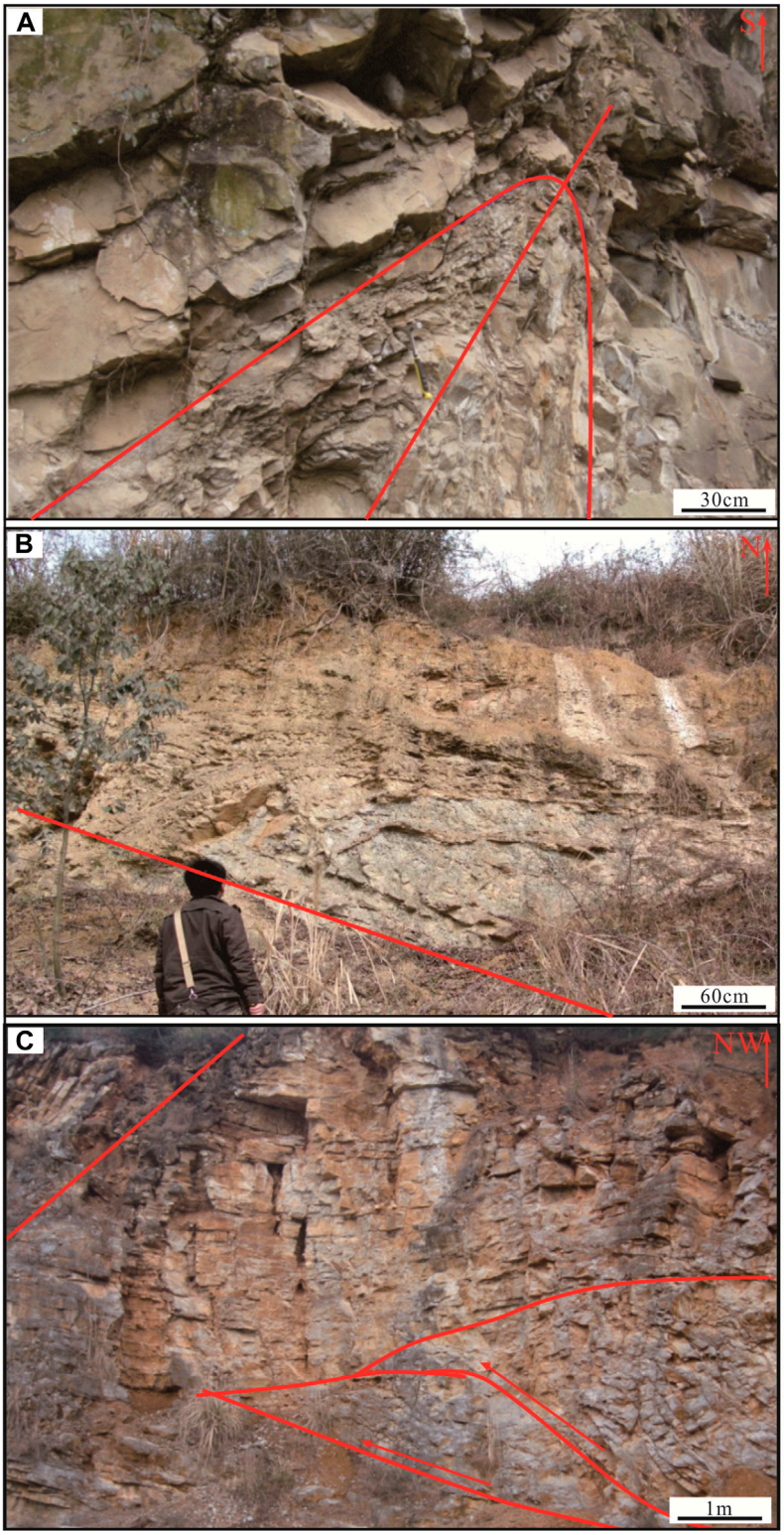

FIGURE 8
Principal structural styles of the thrust overthrust system. **(A)** Reversed syncline structural style; **(B)** Fault-bend fold structural style; **(C)** Thrust wedge structural style.

On the contrary, the subsidiary faults primarily serve a regulatory function. As a result, the trends of the main fault and subsidiary faults are generally opposite. Thrust-up structures manifest as a series of fault blocks on the plane, favoring the creation of fault block traps. Such structures often appear in clusters and are associated with duplex structures (Figure 7B).

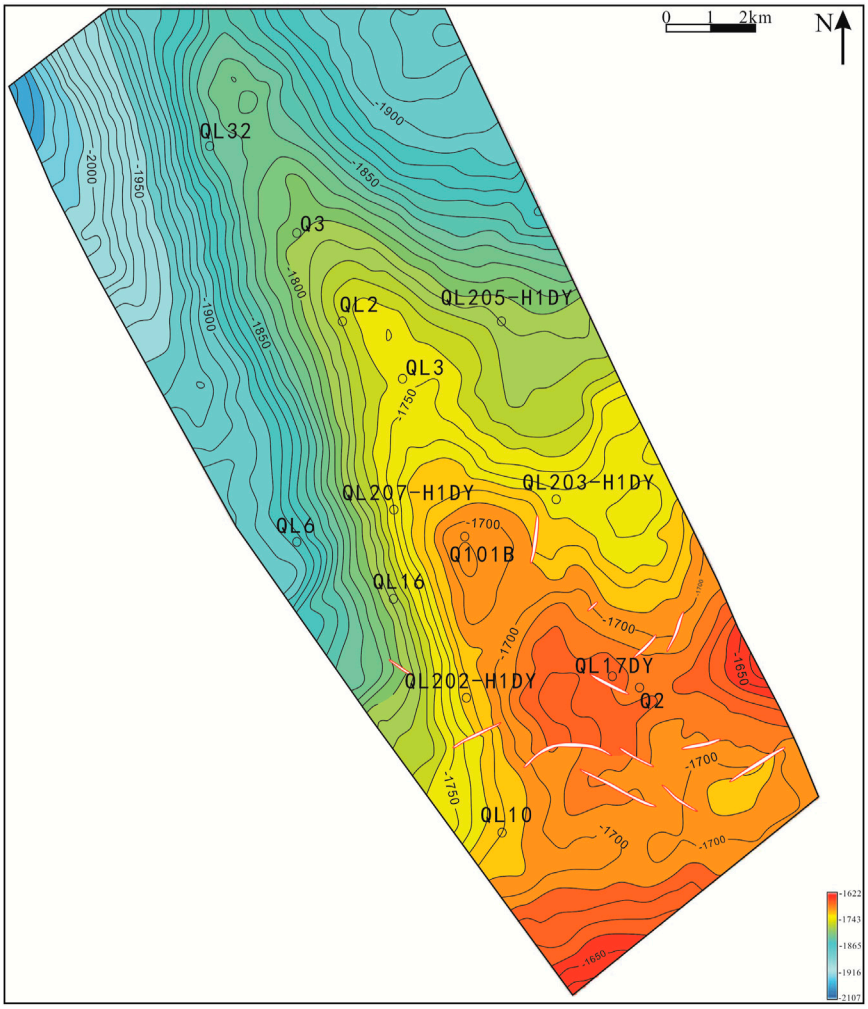

FIGURE 9
Structural map (T0) of the second Member of the Shaximiao Formation in the Qiulin structure.

4.4.2.2 Compression and over-thrusting tectonic system

During the Himalayan period, the intense collision between the Indian and Eurasian Plate led to vigorous compression in the northern Longmenshan (Thingbaijam et al., 2009). This compression profoundly reworked the extensively established structural patterns from the Indosinian-Yanshan period. Rock layers underwent renewed deformation and displacement, resulting in a more intricate network of faults and ultimately shaping the current structural configuration. In contrast, the shallow basin areas of the foreland belt mainly experienced vertical uplift effects, with relatively minor tectonic deformation. These areas largely inherited the earlier structural styles.

Duplex structures are commonly observed in the northern Longmenshan's thrust belt and hinterland areas. They are most pronounced in seismic profiles, with limited outcrop expression. These structures feature hanging-wall and footwall thrust faults. This structural pattern involves a series of imbricate thrust faults forming duplex structures. The study area predominantly inherits the thrust-up structural pattern generated by gravity sliding, modified under later compressional tectonic influences. In the northern Longmenshan hinterland, these structures are predominantly seen within the Lower Triassic and underlying formations at the front edge of the thrust zone (Figure 7B).

Reverted anticline structural style: At the Tianjingshan observation area, a surface outcrop of a reverted anticline has been identified. The exposed strata in the core of the anticline belong to the Cambrian system. The orientation of the left limb, as shown in Figures 8A 315°∠40°, while the orientation of the right limb is 292°∠87°.

Fault-bend fold structural style: A common structural style observed in orogenic and fault zones, it consists of three components: the lower fault plane, fault slope, and upper fault plane (Jiang et al., 2020). The fault-bend fold initiates above the fault slope and deforms into a folding pattern as it progresses. If the deformation continues, it may lead to the development of a thrust fault at the hinge area of the fold. In the deeper parts of the study area, the predominant structural style is the fault-bend fold. Near the Erliangmiao area, a small-scale fault-bend fold is observed in the Shaximiao Formation. The hinterland structural style appears in the core of the Tianjingshan structure. The occurrence of the fault plane,

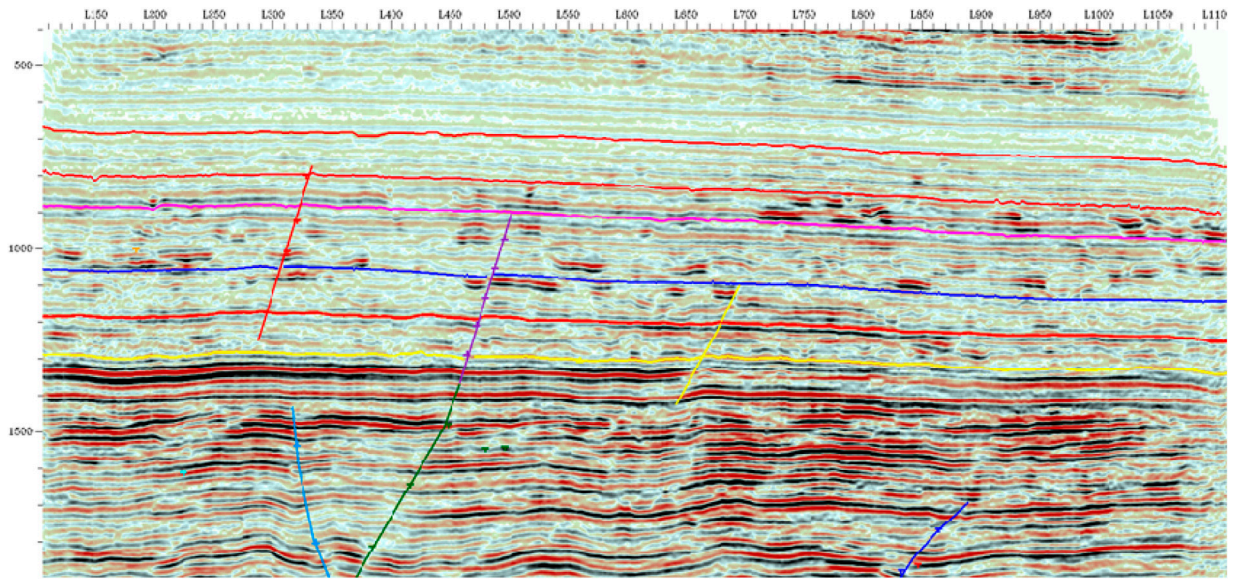

FIGURE 10
Typical fault interpretation profile of the Qiulin area.

the frontal limb, and the rear limb is 180°∠46°, 325°∠35°, and 192°∠14°, respectively (Figure 8B).

The extrusion wedge structural style: The development process of the extrusion wedge generally takes two forms (Sang et al., 2017). The first form involves the development of an extrusion wedge under early extensional stress conditions. During this period, normal faulting activity results in the deposition of syn-rift sedimentary strata within the fault basin. After the cessation of normal faulting, it experiences continuous sedimentation. As extensional stresses transition to compressional stresses, the previously active normal faults reverse and form thrust faults. This change in tectonic stress leads to the development of an extrusion wedge, altering the earlier structural pattern. The second form involves the development of an extrusion wedge through rock brittle failure under compressional stress conditions. This usually results in the formation of two conjugate reverse faults with opposite orientations. In cross-sectional view, these two conjugate reverse faults enclose a wedge-shaped block, which converges and merges at the tip of the wedge-shaped block. The sliding movement along the boundary faults propels the wedge-shaped block forward and induces folding in the overlying strata. During field geological investigations, a detachment wedge of two fault blocks was identified in the hanging wall of the northwest fault at Wenxingchang (Figure 8C).

Additionally, the study area also exhibits frontal (rear) breakout structural styles and crenulated structural styles. The frontal or rear breakout structural style occurs within a compressional environment, especially in association with fault-related folding of the frontal strata, leading to fracturing and the development of breakout structures. These structures primarily serve for stress transmission and release. Crenulated structures generally occur within the gravity-sliding foreland belt or the interior of thrust structures. They are characterized by parallel and overlapping thrust faults stacked together, with the fault planes typically oriented in parallel.

4.4.3 3D detailed structural interpretation

Based on the latest 3D seismic and logging data in the study area and previous research findings, the application of well-seismic correlation, various cross-sections, and profile integration has solidified the understanding of the structural characteristics in the Qiulin area. The Qiulin structure is primarily a single-fault structure that has undergone overall inherited development. It is situated on the down-dip slope of the northern Sichuan ancient depression. Currently, the surface expression of the structure appears as a northwest-oriented nasal-shaped uplift with some localized high points. The hinterland structure exhibits an overall northwest-oriented slope, although there are variations in the different rock layers. Northwest-oriented anticlinal structures, similar to the surface features, primarily characterize the second Member.

Additionally, the slopes on the eastern and western flanks of the structure are steeper. Multiple local structural highs have developed on the anticlinal structure and its flanks, potentially serving as favorable areas for oil and gas accumulation. The highest part is a small-scale syncline located west of well QL17. This syncline exhibits a relatively large closure area, estimated to be approximately 2.3 km^2 (Figure 9).

The folding within the Shaximiao Formation of the Qiulin Structure is not intensely pronounced, exhibiting relatively gentle structural characteristics. Local occurrences of small-scale normal faults can be observed. In the southern parts of the study area, multiple normal faults extend downward to the base of the Shaximiao Formation, primarily oriented in a northwestern direction. The length of these faults ranges from 0.8 to 2.2 km. However, in the northern parts, the development of faults is not significant (Figure 10). Therefore, the Qiulin structure is characterized by a northwestern tilting nose-shaped structure. Within the Shaximiao Formation, there is a predominant development of normal faults. This suggests that

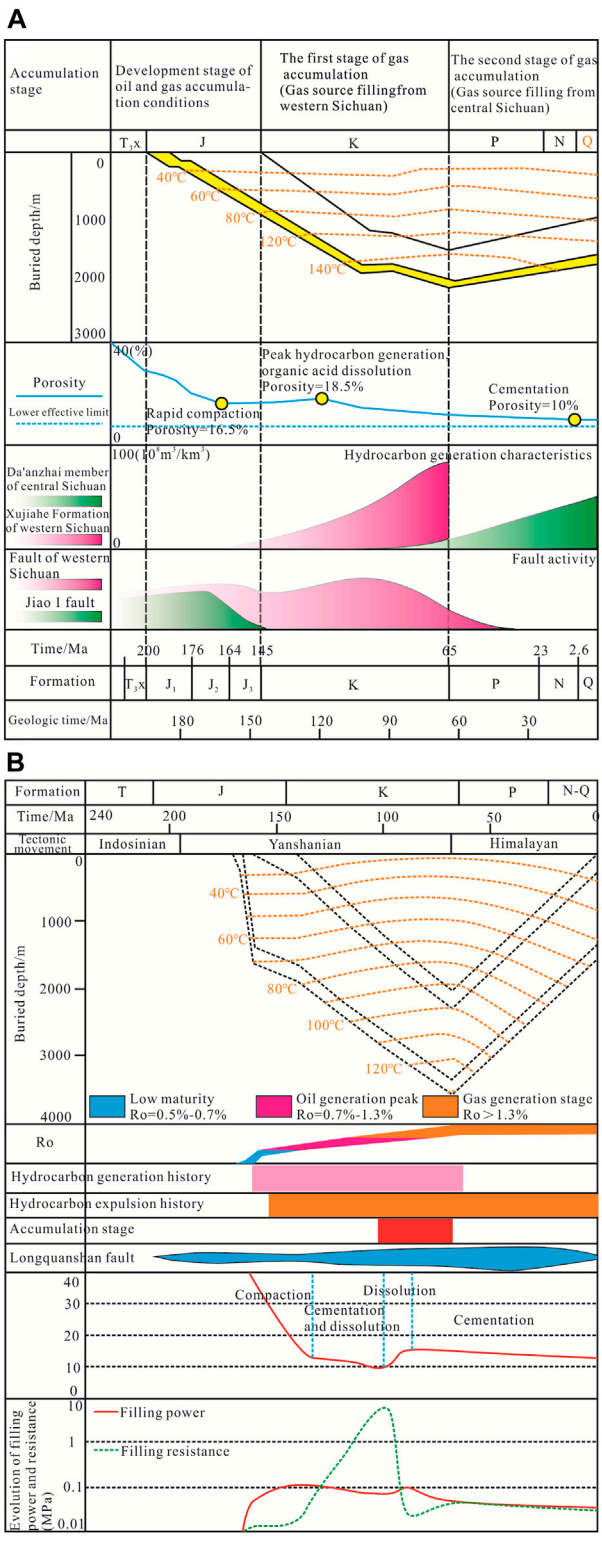

FIGURE 11
Temporal correlation of key factors in the gas reservoir formation. **(A)** The second Member of the Shaximiao Formation; **(B)** The 1st of the Shaximiao Formation.

the area was subjected to extensional tectonic forces, indicating its presence within a gravitational sliding tectonic subsidence zone during the Yanshan period. The area experienced extensional tectonic stress, resulting in a predominant uplift of the strata.

5 Discussion

5.1 Impact of tectonic movement on thermal evolution and distribution of source rocks

The Xujiahe Formation in the Early Jurassic is characterized by its multiple layers, significant sedimentary thickness, high organic matter abundance, and substantial hydrocarbon generation potential. It serves as the most crucial source rock of the Shaximiao Formation. The peak of hydrocarbon generation occurs during the Early Cretaceous to Paleogene. During the initial deposition of the Shaximiao Formation (the Middle Jurassic), hydrocarbon generation from the source rocks in the western Sichuan Basin did not reach its peak. During the Late Jurassic to Cretaceous period, abundant hydrocarbon generation occurred from the Xujiahe Formation source rocks in the western Sichuan Basin. Reservoir dissolution processes took place during this period. The frequent activity of the western Sichuan faults facilitated the migration and accumulation of hydrocarbons in deeper reservoirs, marking the first period of gas accumulation in the Shaximiao Formation. From the Cretaceous period to the present, the Da'anzhai Member of the Ziliujing Formation gradually entered the hydrocarbon generation window and began to produce a significant amount of hydrocarbons. At the same time, it was influenced by small-scale faults developed within the Jurassic strata. As the oil and gas concentration reached a certain level, there was significant intra-layer migration and regional accumulation. This led to subsequent adjustments in the gas reservoir during its later periods (Oliveira et al., 2021). Under the same sedimentary and structural background, differences in the fluid charging history can result in significant variations in the pressure evolution process of different gas reservoirs. The temporal relationship between the uplift and erosion of stratigraphic layers and the timing of oil and gas charging in the study area significantly impacts the pressure formation and evolution process of gas reservoirs (Figures 11A, B). The gas reservoirs in the Qiulin area are primarily charged by hydrocarbons from the source rock of the Xujiahe Formation. During the Late Jurassic to Cretaceous period, it generated substantial hydrocarbons. As stratigraphic layers underwent uplift and erosion, leading to a reduction in pressure, hydrocarbons migrated towards lower-potential-energy sandstone reservoirs (Li et al., 2009; Fang et al., 2011; Wu et al., 2012; Wood and Hazra, 2018). Dissolved-state natural gas began to exsolve and accumulate within the fluvial sandstone reservoirs of the Shaximiao Formation. In this process, the dynamic equilibrium between erosion-driven unloading and pressure reduction and hydrocarbon-charging-induced pressure increase, leads to the characteristic of these gas reservoirs maintaining near-normal pressure conditions.

5.2 Impact of tectonic movement on gas migration

The formation and evolution of the Sichuan Basin have undergone multiple tectonic movements, resulting in a complex system of faults and fractures, which serve as the dominant pathways

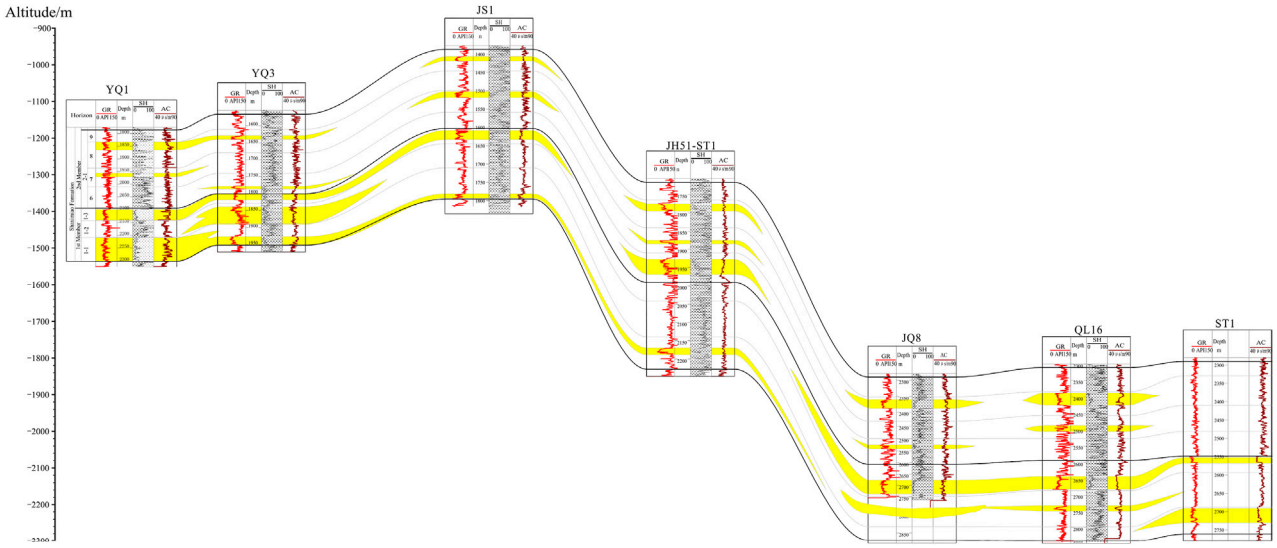

FIGURE 12
Interpreted correlations in composite cross section of 7 wells gas reservoir in the Shaximiao Formation.

for oil and gas migration (Xu and Gao, 2020; Li et al., 2021; Shan et al., 2021; Li et al., 2022). Therefore, faults and fractures are the dominant pathways for gas migration of the Shaximiao Formation reservoir in the Qiulin area. During the Yanshan period, the shallow layers (Xujiahe-Shaximiao Formations) were affected by a series of small-scale normal faults. In the peak hydrocarbon expulsion period of the Cretaceous to Paleogene, gas migrated along these minor faults and was preserved in the Shaximiao Formation reservoir.

The gas reservoirs are considered to be long-distance migrated accumulations (Zhu et al., 2013; Zhang et al., 2020; Zhang et al., 2022). The fault network plays a crucial role in migrating and accumulating gas from distant source rocks. The fault systems in the Shaximiao Formation can be classified into three types: 1) Faults that act as conduits between the Xujiahe and Shaximiao Formations; 2) Faults that facilitate communication between the Ziliujing or Lianggaoshan and other Formations; 3) Internal faults in the Shaximiao Formation. The first two categories are hydrocarbon-source faults, connecting the coal-bearing hydrocarbon source rocks of the Xujiahe Formation and the lacustrine hydrocarbon source rocks of the Lower Jurassic.

The hydrocarbon-source faults are characterized by their larger scale and longer extension distances in the western Sichuan Basin (Zhu et al., 2013; Zhang et al., 2023). These faults were generally active during the deposition of the Xujiahe to the Suining Formations. Some of these faults have remained active even in later periods. Due to the absence of Lower Jurassic hydrocarbon-source rocks in the western Sichuan area, only the gas generated from the Xujiahe Formation efficiently migrated within long-lived faults to the Shaximiao Formation. This gas preferentially filled the lower fluvial sandstones, resulting in an overall gas-rich reservoir in the 1st Member and the 1st layer of the second Member. However, varying degrees of gas enrichment in different sandstone layers within different areas indicate differences in gas migration and accumulation through the faults. The characteristics of hydrocarbon-source faults determine the overall enrichment gas features in the Shaximiao Formation. However, the small-scale faults also contribute to the localized variations in enrichment. Internal faults facilitate the connection between the upper and lower sandstone layers. The lower layer is enriched with natural gas from hydrocarbon-source faults, while the upper layer lacks such enrichment. However, gas exchange has occurred over time due to the communication effect of internal faults and the influence of later tectonic activity. In conclusion, the varying distribution of internal faults and their different roles in gas migration has led to the vertical enrichment of natural gas in multiple sandstone layers in the Shaximiao Formation (Figure 12).

5.3 Impact of tectonic movement on gas preservation

In the study area, the reservoir of the Shaximiao Formation mainly consists of distributary channel sands and river sands of the delta front. The overlying Suining Formation acts as the regional cap rock, and the Cretaceous Guankou Formation provides an extensive sealing layer distribution. This ensures the effective containment of oil and gas within the sandstone reservoirs, providing high-quality cap rock for reservoir accumulation (Wang and Shi, 2019; Cai, 2020; Fan et al., 2022; Wang et al., 2022). During the Yanshan period, the Songpan-Ganzi Plateau and the hinterland of the Longmenshan experienced a renewed uplift following the Indosinian tectonic movement. At this time, the frontal thrust zone of the Longmenshan overthrust belt exhibited a gravity-sliding structural system. During this period, the collision of the overthrust belt with the rift basin formed during the Indosinian period led to the strata's bending and subsidence, resulting in a depression. During this time, fluvial-dominated sedimentation was predominant, with the sand bodies favoring natural gas accumulation. Furthermore, due to its extensional tectonic setting, a series of small normal faults formed, providing conduits for the migration of hydrocarbons from underlying

source rocks. During the Middle-Late Yanshan and the Himalayan period, tectonic movements along these faults effectively charged the tight gas reservoirs of the Shaximiao Formation.

6 Conclusion

Based on the data from cores, outcrops, mud logging, logging, seismic interpretation, and burial history analysis, this paper takes of the tight gas reservoir in the Jurassic Shaximiao Formation in the Qiulin structure as an example. Through the study of source rocks, sedimentation, reservoir, and structural characteristics, this paper elucidates the impact of the Yanshan-Himalayan tectonic movement in the northern Longmenshan on the gas accumulation of the Shaximiao Formation. The following conclusions have been primarily drawn.

(1) Structural characteristics in the northern Longmenshan belt show variations during the Yanshan-Himalayan period. During the Yanshan period, the area was a unified unit influenced by gravity-sliding tectonics, divided into four zones: 'Uplifted Zone,' 'Slope Belt,' 'Foreland Belt,' and 'Depression Zone', known as the "Three Zones and One Belt". In the Himalayan period, vertical uplift led to complex structures, including duplex, overturned anticlines, fault-bend folds, and thrust wedges.
(2) Sedimentary history in the northern Longmenshan can be summarized as "rapid subsidence-slow subsidence-rapid uplift" phases. Early to Middle Yanshan saw rapid subsidence, followed by sustained slow subsidence. Late Yanshan witnessed increased tectonic activity and rapid uplift, continuing into the early Himalayan movement, followed by erosion.
(3) Faults and favorable reservoirs influence gas accumulation in the Qiulin area. The depocenter area favors gas accumulation in the gravitational sliding structural system. The coupling relationship between the foreland belt and the depocenter area facilitates the development of sedimentary environments, such as river-lake systems conducive to gas storage. Simultaneously, the depocenter area benefits from extensional tectonic activity that forms tensional normal faults, facilitating the migration of oil and gas. During the Himalayan period, compressional forces dominated, primarily modifying pre-existing traps or structures to varying degrees across different areas.

Data availability statement

The original contributions presented in the study are included in the article/Supplementary material, further inquiries can be directed to the corresponding author.

Author contributions

YY: Conceptualization, Data curation, Formal Analysis, Investigation, Methodology, Software, Supervision, Writing–original draft, Writing–review and editing. XL: Formal Analysis, Resources, Validation, Writing–original draft, Writing–review and editing. ZW: Software, Supervision, Writing–review and editing. WY: Conceptualization, Resources, Writing–review and editing.

Acknowledgments

YY and XL contributed to the paper's formal analysis, writing, reviewing, editing, and revising. ZW and WY contributed to the paper's editing and revising.

Conflict of interest

Authors YY and XL were employed by PetroChina Southwest Oil & Gasfield Company.

The remaining authors declare that the research was conducted in the absence of any commercial or financial relationships that could be construed as a potential conflict of interest.

Publisher's note

References

Alsalem, O. B., Fan, M. J., and Xie, X. Y. (2017). Late Paleozoic subsidence and burial history of the Fort Worth basin. *AAPG Bull.* 101 (11), 1813–1833. doi:10.1306/01251716016

Braunagel, M. J., Griffith, W. A., Biek, R. F., Hacker, D. B., Rowley, P. D., Malone, D. H., et al. (2023). Structural relationships across the sevier gravity slide of Southwest Utah and implications for catastrophic translation and emplacement processes of long runout landslides. *Geochem. Geophy. Geosy.* 24 (5), e2022GC010783. doi:10.1029/2022GC010783

Bretas, E. M., Leger, P., and Lemos, J. V. (2012). 3D stability analysis of gravity dams on sloped rock foundations using the limit equilibrium method. *Comput. Geotech.* 44, 147–156. doi:10.1016/j.compgeo.2012.04.006

Cai, M. F. (2020). Key theories and technologies for surrounding rock stability and ground control in deep mining. *J. Min. Strata Control Eng.* 2 (3), 033037. doi:10.13532/j.jmsce.cn10-1638/td.20200506.001

Dai, J., Ni, Y., Zou, C., Tao, S., Hu, G., Hu, A., et al. (2009). Stable carbon isotopes of alkane gases from the Xujiahe coal measures and implication for gas-source correlation in the Sichuan Basin, SW China. *Org. Geochem.* 40 (5), 638–646. doi:10.1016/j.orggeochem.2009.01.012

Dai, J. X., Liao, F. R., and Ni, Y. Y. (2013). Discussions on the gas source of the Triassic Xujiahe Formation tight sandstone gas reservoirs in Yuanba and Tongnanba, Sichuan Basin: an answer to Yinfeng et al. *Petrol. explor. Dev.* 40 (2), 250–256. doi:10.11698/PED.2013.02.17

Dai, J. X., Ni, Y. Y., Qin, S. F., Huang, S. P., Peng, W. L., and Han, W. X. (2018). Geochemical characteristics of ultra-deep natural gas in the Sichuan Basin, SW China. *Petrol. explor. Dev.* 45 (4), 619–628. doi:10.1016/s1876-3804(18)30067-3

Deng, B., Liu, S. G., Jiang, L., Zhao, G. P., Huang, R., Li, Z. W., et al. (2018). Tectonic uplift of the Xichang Basin (SE Tibetan Plateau) revealed by structural geology and thermochronology data. *Basin Res.* 30, 75–96. doi:10.1111/bre.12243

Deng, B., Liu, S. G., Liu, S., Jansa, L., Li, Z. W., and Zhong, Y. (2013). Progressive indosinian NS deformation of the jiaochang structure in the songpan-ganzi fold-belt, western China. *PLoS One* 8 (10), e76732. doi:10.1371/journal.pone.0076732

Deng, P., Fang, C., Deng, M. Z., and Zhao, L. (2021). New insights into structural characteristics in central-northern Longmen Mountains: implications for multiple-decollement deformation. *Petrol. Geol. Exp.* 43 (1), 45–55. doi:10.11781/sysydz202101045

Ding, X., Li, Z. Q., Li, J. N., Li, H. K., Chen, X., Liu, R., et al. (2022). Age limit of diabase dyke intrusion in Tangwangzhai-Yangtianwo compound syncline in the northern section of Longmen Mountain, western Sichuan Province. *Geol. Bull. China* 41 (8), 1409–1416. doi:10.12097/j.issn.1671-2552.2022.08.008

Fan, C. H., Xie, H. B., Li, H., Zhao, S. X., Shi, X. C., Liu, J. F., et al. (2022). Complicated fault characterization and its influence on shale gas preservation in the southern margin of the Sichuan Basin, China. *Lithosphere* 2022 (12), 8035106. doi:10.2113/2022/8035106

Fang, Y., Liao, Y., Wu, L., and Geng, A. (2011). Oil-source correlation for the paleo-reservoir in the Majiang area and remnant reservoir in the Kaili area, South China. *J. Asian Earth Sci.* 41, 147–158. doi:10.1016/j.jseaes.2011.01.012

Freeman, K. H., Hayes, J. M., Trendel, J. M., and Albrecht, P. (1990). Evidence from carbon isotope measurements from diverse origins of sedimentary hydrocarbons. *Nature* 343, 254e256. doi:10.1038/343254a0

Gao, Z., Fan, Y., Xuan, Q., and Zheng, G. (2020). A review of shale pore structure evolution characteristics with increasing thermal maturities. *Adv. Geo-Energy Res.* 4 (3), 247–259. doi:10.46690/ager.2020.03.03

Gu, M. X., Xie, R. H., and Jin, G. W. (2021). A machine-learning based quantitative evaluation of the fluid components on T-2-D spectrum. *Mar. Petrol. Geol.* 134, 105353. doi:10.1016/j.marpetgeo.2021.105353

Gunderson, K. L., Anastasio, D. J., Pazzaglia, F. J., and Kodama, K. P. (2018). Intrinsically variable blind thrust faulting. *Tectonics* 37 (5), 1454–1471. doi:10.1029/2017TC004917

He, S., Qin, Q. R., Li, H., and Zhao, S. X. (2022a). Geological characteristics of deep shale gas in the Silurian Longmaxi Formation in the southern Sichuan Basin, China. *Front. Earth Sci.* 9, 818543. doi:10.3389/feart.2021.818155

He, S., Qin, Q. R., Li, H., and Wang, S. L. (2022b). Deformation differences in complex structural areas in the southern Sichuan Basin and its influence on shale gas preservation: a case study of Changning and Luzhou area. *Front. Earth Sci.* 9, 818155. doi:10.3389/feart.2021.818534

Huang, C., Zhou, X. J., Shen, Y. W., Wen, X., Zhai, M. L., and Tan, X. C. (2022). Stratigraphic age distribution and sedimentary filling of the Guanwushan Formation in the northern segment of Longmenshan Mountains, and its palaeogeographic significance. *Acta Geol. Sin.* 96 (7), 2255–2271. doi:10.19762/j.cnki.dizhixuebao.2022056

Jiang, D. Q., Wang, M. M., Song, G. H., Yan, B., and Feng, W. (2020). Transition from fault-propagation folds to fault-bend folds determined by along-strike variations of structural styles and fault displacement-distance relationships: the Sumatou anticline, Sichuan Basin, China. *J. Struct. Geol.* 131, 103951. doi:10.1016/j.jsg.2019.103951

Jin, W. Z., Tang, L. J., Yang, K. M., Wan, G. M., Lu, Z. Z., and Yu, Y. X. (2009). Transfer zones within the Longmen Mountains thrust belt, SW China. *Geosci. J.* 13 (1), 1–14. doi:10.1007/s12303-009-0001-9

Jin, W. Z., Tang, L. J., Yang, K. M., Wan, G. M., Lu, Z. Z., and Yu, Y. X. (2010). Structural styles of longmen mountain thrust belt, SW China. *J. Earth Sci.* 21 (1), 19–31. doi:10.1007/s12583-010-0010-7

Lan, S. R., Song, D. Z., and Li, Z. L. (2021). Experimental study on acoustic emission characteristics of fault slip process based on damage factor. *J. Min. Strata Control Eng.* 3 (3), 033024. doi:10.13532/j.jmsce.cn10-1638/td.20210510.002

Lei, Y. L., Jia, C. Z., Li, B. L., Wei, G. Q., Chen, Z. X., and Shi, X. (2012). Meso-Cenozoic tectonic events recorded by apatite fission track in the northern Longmen-Micang Mountains region. *Acta Geol. sin.-eng. Ed.* 81 (1), 153–165. doi:10.1111/j.1755-6724.2012.00618.x

Li, D., Hong, F. L., Shao, Y. J., Jia, Y. P., Yong, Q. C., Yuan, F. C., et al. (2009). New carbon isotope stratigraphy of the Ediacaran-Cambrian boundary interval from SW China: implications for global correlation. *Geol. Mag.* 146, 465e484. doi:10.1017/S0016756809006268

Li, H., Tang, H. M., Qin, Q. R., Zhou, J. L., Qin, Z. J., Fan, C. H., et al. (2019a). Characteristics, formation periods and genetic mechanisms of tectonic fractures in the tight gas sandstones reservoir: a case study of Xujiahe Formation in YB area, Sichuan Basin, China. *J. Petrol. Sci. Eng.* 178, 723–735. doi:10.1016/j.petrol.2019.04.007

Li, H., Tang, H. M., Qin, Q. R., Wang, Q., and Zhong, C. (2019b). Effectiveness evaluation of natural fractures in Xujiahe Formation of Yuanba area, Sichuan basin, China. *Arab. J. Geosci.* 12 (6), 194. doi:10.1007/s12517-019-4292-5

Li, H., Wang, Q., Qin, Q. R., and Ge, X. Y. (2021). Characteristics of natural fractures in an ultradeep marine carbonate gas reservoir and their impact on the reservoir: a case study of the Maokou Formation of the JLS Structure in the Sichuan Basin, China. *Energy Fuel* 35 (16), 13098–13108. doi:10.1021/acs.energyfuels.1c01581

Li, J., Li, H., Yang, C., Ren, X. H., and Li, Y. D. (2023). Geological characteristics of deep shale gas and their effects on shale fracability in the Wufeng–Longmaxi Formations of the southern Sichuan Basin, China. *Lithosphere* 2023 (1), 4936993. doi:10.2113/2023/4936993

Li, J., Li, H., Yang, C., Wu, Y. J., Gao, Z., and Jiang, S. L. (2022). Geological characteristics and controlling factors of deep shale gas enrichment of the Wufeng-Longmaxi Formation in the southern Sichuan Basin, China. *Lithosphere* 2022 (12), 4737801. doi:10.2113/2022/4737801

Liu, K. X., Chen, J. F., Fu, R., Wang, H., Luo, B., Chen, Z. Y., et al. (2023). Distribution characteristics and controlling factors of helium-rich gas reservoirs. *Gas. Sci. Eng.* 110, 204885. doi:10.1016/j.jgsce.2023.204885

Liu, S. G., Yang, Y., Deng, B., Zhong, Y., Wen, L., Sun, W., et al. (2021). Tectonic evolution of the Sichuan Basin, southwest China. *Earth Sci. Rev.* 213, 103470. doi:10.1016/j.earscirev.2020.103470

Lu, X. L., Li, M. J., Wei, T. Q., Wu, C. J., Tang, Y. J., Wang, X. J., et al. (2022). Composition of light hydrocarbons in Jurassic tight oils in the central Sichuan Basin, China: origin and source rock correlation. *J. Petrol. Geol.* 45 (2), 163–177. doi:10.1111/jpg.12811

Luo, L., Jia, D., Qi, J. F., Wei, G. Q., and Deng, F. (2013). Tectono-sedimentary evolution of the late triassic Xujiahe Formation in the Sichuan Basin. *Acta Geol. Sin-Eng. Ed.* 87 (6), 1554–1568. doi:10.1111/1755-6724.12159

Lyu, Q., Wang, W. M., Jiang, Q. C., Yang, H. F., Deng, H., Zhu, J., et al. (2023). Basement reservoirs in China: distribution and factors controlling hydrocarbon accumulation. *Minerals* 13 (8), 1052. doi:10.3390/min13081052

Ma, D., Zhang, Z. J., Zhou, C. M., Cheng, D. W., Hong, H. T., Meng, H., et al. (2023). Element geochemical characteristics and geological significance of mudstones from the middle jurassic Shaximiao Formation in Sichuan Basin, southwest China. *ACS Omega* 8 (33), 29979–30000. doi:10.1021/acsomega.3c01496

Martins, G., Ettensohn, F. R., and Knutsen, S. M. (2023). Use of backstripping in the Triassic-Middle Jurassic, south-central Barents Sea shelf succession to understand regional tectonic mechanisms and structural responses. *Tectonophysics* 853, 229797. doi:10.1016/j.tecto.2023.229797

Mu, H., Yan, D. P., Qiu, L., Yang, W.-X., Kong, R.-Y., Gong, L.-X., et al. (2019). Formation of the late triassic Western sichuan foreland basin of the qinling orogenic belt, SW China: sedimentary and geochronological constraints from the Xujiahe Formation. *J. Asian Earth Sci.* 183, 103938. doi:10.1016/j.jseaes.2019.103938

Oliveira, G. P., Rodrigues, T. N. E., and Lie, K. A. (2021). GAWPS: a MRST-based module for wellbore profiling and graphical analysis of flow units. *Adv. Geo-Energy Res.* 6 (1), 38–53. doi:10.46690/ager.2022.01.04

Petermann, H., Lyson, T. R., Miller, I. M., and Hagadorn, J. W. (2022). Crushed turtle shells: proxies for lithification and burial-depth histories. *Geosphere* 18 (5), 1524–1537. doi:10.1130/GES02513.1

Sang, M., Xiao, W. J., Bakirov, A., Orozbaev, R., Sakiev, K., and Zhou, K. F. (2017). Oblique wedge extrusion of UHP/HP complexes in the Late Triassic: structural analysis and zircon ages of the Atbashi Complex, South Tianshan, Kyrgyzstan. *Int. Geol. Rev.* 59 (10), 1369–1389. doi:10.1080/00206814.2016.1241163

Shan, S. C., Wu, Y. Z., Fu, Y. K., and Zhou, P. H. (2021). Shear mechanical properties of anchored rock mass under impact load. *J. Min. Strata Control Eng.* 3 (4), 043034. doi:10.13532/j.jmsce.cn10-1638/td.20211014.001

Thingbaijam, K. K. S., Chingtham, P., and Nath, S. K. (2009). Seismicity in the North-west frontier province at the Indian-Eurasian Plate convergence. *Seismol. Res. Lett.* 80 (4), 599–608. doi:10.1785/gssrl.80.4.599

Wang, C., and Shi, G. (2019). Redox condition and organic carbon accumulation mechanism in the Cryogenian Nanhua Basin, South China: insights from iron chemistry and sulfur, carbon, oxygen isotopes of the Datangpo Formation. *Adv. Geo-Energy Res.* 3 (1), 67–75. doi:10.26804/ager.2019.01.05

Wang, Z., Hao, C., Jin, H., Cui, J., Wu, X., Bo, D., et al. (2023). Geochemical characteristics and hydrocarbon generation potential of main source rocks in the Upper Triassic Xujiahe Formation, Sichuan Basin, China. *Front. Earth Sci.* 11, 1233959. doi:10.3389/feart.2023.1233959

Wang, S. L., Li, H., Lin, L. F., and Yin, S. (2022). Development characteristics and finite element simulation of fractures in tight oil sandstone reservoirs of Yanchang Formation in western Ordos Basin. *Front. Earth Sci.* 9, 823855. doi:10.3389/feart.2021.823855

Wei, T. Q., Zhang, B. J., and Wang, X. J. (2021). Sedimentary characteristics of fluvial facies and analysis of reservoir differences in the second member of Jurassic Shaximiao Formation in Qiulin Area, Sichuan Basin. *Sci. Technol. Eng.* 21 (29), 12438–12446.

Wen, L., Wang, W. Z., Zhang, J., and Luo, B. (2017). Classification of sinian dengying Formation and sedimentary evolution mechanism of gaoshiti-moxi area in central Sichuan Basin. *Acta Petrol. Sin.* 33 (4), 1285–1294.

Wood, D. A., and Hazra, B. (2018). Pyrolysis S2-peak characteristics of Raniganj shales (India) reflect complex combinations of kerogen kinetics and other processes related to different levels of thermal maturity. *Adv. Geo-Energy Res.* 2 (4), 343–368. doi:10.26804/ager.2018.04.01

Wu, L. L., Liao, Y. H., Fang, Y. X., and Geng, A. S. (2012). The study on the source of the oil seeps and bitumens in the Tianjingshan structure of the northern Longmen Mountain structure of Sichuan Basin, China. *Mar. Petrol. Geol.* 37 (1), 147–161. doi:10.1016/j.marpetgeo.2012.05.011

Wu, Z. J., Li, T. F., Ji, S., Zhou, Q., and Tian, H. (2023). Gas generation from coal and coal-measure mudstone source rocks of the Xujiahe Formation in the western sichuan depression, Sichuan Basin. *J. Earth Sci.* 34 (4), 1012–1025. doi:10.1007/s12583-022-1627-z

Xia, L., Liu, Z., Li, W. L., Lu, C. J., Yang, X. G., and Liu, M. J. (2018). Ternary analytic porosity-reduction model of sandstone compaction trend and its significance in petroleum geology: a case study of tight sandstones in Permian Lower Shihezi Formation of Shilijiahan area, Ordos Basin, China. *Petrol. explor. Dev.* 45 (2), 290–301. doi:10.1016/S1876-3804(18)30032-6

Xie, G. Y., Hu, X., Wang, X. L., Yang, T., Tian, Y. Y., Xin, R. Y., et al. (2023). Structural analysis and exploration prospects of nappe-piedmont structural belt in northern Longmenshan area, Sichuan Basin. *Nat. Gas. Explor. Dev.* 46 (1), 11–17. doi:10.12055/gaskk.issn.1673-3177.2023.01.002

Xie, G. Y., Tian, Y. Y., Liu, B., Fan, S. H., Ma, Y. H., and Zhang, Y. L. (2022). Formation conditions and controlling factors of high-quality reservoirs in the middle jurassic Shaximiao Formation of the southwestern Sichuan Basin. *Nat. Gas. Ind.* 42 (7), 45–54. doi:10.3787/j.issn.1000-0976.2022.07.005

Xu, L., Li, Q., Myers, M., and Tan, Y. S. (2022). Effects of bedding direction on brine imbibition in Lower Shaximiao tight sandstone: an NMR analysis. *J. Petrol. Sci. Eng.* 210, 110006. doi:10.1016/j.petrol.2021.110006

Xu, N. Z., and Gao, C. (2020). Study on the special rules of surface subsidence affected by normal faults. *J. Min. Strata. Control Eng.* 2 (1), 011007. doi:10.13532/j.jmsce.cn10-1638/td.2020

Yang, M. Y., Sun, W., Gong, T. T., Zhao, H., Lu, N. Z., Zhao, D. J., et al. (2023b). Characteristics and significance of the "mung bean rock" of the middle triassic leikoupo formation at majiaoba, northern section of longmen mountains, sichuan. *Min. Petrol.* 43 (2), 121–131. doi:10.19719/j.cnki.1001-6872.2023.02.12

Yang, W. W., Zhang, C., Shi, X. L., Cui, Y. J., and Zhang, Z. S. (2023c). Reconstruction of LWD-NMR T2 water spectrum and fluid recognition based on microscopic pore structure constraints. *Gas. Sci. Eng.* 221, 211386. doi:10.1016/j.geoen.2022.211386

Yang, Y., Li, Z. Q., and Long, W. (2022). New exploration field of piedmont complex fault-fold belt in the northern Longmen Mountain, Sichuan, China. *J. Chengdu Univ. Technol.* 49 (4), 414–423. doi:10.3969/j.issn.1671-9727.2022.04.02

Yang, Y. M., Bai, X. L., Yi, H. Y., Liu, R., Ma, H. L., Han, S., et al. (2023a). Progress and potential of natural gas exploration in the complex tectonic belt of Longmen Mountain: learning from drilling achievements of Well Hongxing 1. *Nat. Gas. Ind.* 43 (2), 1–14. doi:10.3787/j.issn.1000-0976.2023.02.001

Yang, Y. M., Chen, C., Wen, L., Chen, X., Liang, H., Liu, R., et al. (2018). Characteristics of buried structures in the northern Longmenshan mountains and its significance to oil and gas exploration in the Sichuan Basin. *Nat. Gas. Ind.* 38 (8), 8–15. doi:10.3787/j.issn.1000-0976.2018.08.002

Yu, G., Liu, C., Zhang, L., and Fang, L. (2021). Parameter sensitivity and economic analyses of an interchange-fracture enhanced geothermal system. *Adv. Geo-Energy Res.* 5 (2), 166–180. doi:10.46690/ager.2021.02.06

Zhang, D. D., Li, S. J., and Zhang, X. (2020). Experimental study on mining fault activation characteristics by a distributed optical fiber system. *J. Min. Strata Control Eng.* 2 (1), 013018. doi:10.13532/j.jmsce.cn10-1638/td.2020.01.010

Zhang, P. S., Xu, D. Q., and Fu, X. (2022). Evaluation of hydraulic conductivity based on fault confinement studies. *J. Min. Strata Control Eng.* 4 (2), 023033. doi:10.13532/j.jmsce.cn10-1638/td.20211215.001

Zhang, T. T., Wang, H., Yue, Y., Huang, C. Y., and Zhang, L. W. (2009). Cenozoic subsidence features of Beitang Sag and relationship with tectonic evolution. *J. Earth Sci.* 20 (4), 746–754. doi:10.1007/s12583-009-0061-9

Zhang, Z. H., Wang, H. Y., Yang, X. B., Su, X. Y., Tian, Y. C., Wang, J., et al. (2023). Seismic interpretation and geological evaluation of hydrocarbon source rocks in volcanic-rich continental lacustrine rift basins: a case study of the Lower Cretaceous Yingcheng Formation from the Changling Fault Depression in the Songliao Basin, NE China. *Geoenergy Sci. Eng.* 221, 211397. doi:10.1016/j.geoen.2022.211397

Zhu, B. Y., Meng, J. H., Pan, R. F., Hu, H. Y., Song, C., Zhu, Z. P., et al. (2023). New insights into the evaluation criteria for high-quality deep marine shale gas reservoirs in the Longmaxi formation: evidence from organic matter pore development characteristics. *Front. Ecol. Evol.* 11, 1138991. doi:10.3389/fevo.2023.1138991

Zhu, G. Y., Yang, H. J., Zhang, B., Su, J., Zhang, C., Zhang, K., et al. (2013). Ultra-long distance migration of hydrocarbon. *Acta Petrol. Sin.* 29 (9), 3192–3212.

Zhu, Y. P., and Li, P. (2019). One improved burial history recovery method and computer model establishment. *J. Petrol. Explor. Prod. Te.* 9 (1), 75–86. doi:10.1007/s13202-018-0502-z